Huanchun Cui[1]
Prashanta Dutta[2]
Cornelius F. Ivory[1]

[1]School of Chemical Engineering and Bioengineering, Washington State University, Pullman, WA, USA
[2]School of Mechanical and Materials Engineering, Washington State University, Pullman, WA, USA

Received August 23, 2006
Revised September 28, 2006
Accepted September 28, 2006

Research Article

Isotachophoresis of proteins in a networked microfluidic chip: Experiment and 2-D simulation

This paper reports both the experimental application and 2-D simulation of ITP of proteins in a networked microfluidic chip. Experiments demonstrate that a mixture of three fluorescent proteins can be concentrated and stacked into adjacent zones of pure protein under a constant voltage of 100 V over a 2 cm long microchannel. Measurements of the isotachophoretic velocity of the moving zones demonstrates that, during ITP under a constant voltage, the zone velocity decreases as more of the channel is occupied by the terminating electrolyte. A 2-D ITP model based on the Nernst–Planck equations illustrates the stacking and separation features of ITP using simulations of three virtual proteins. The self-sharpening behavior of ITP zones dispersed by a T-junction is clearly demonstrated both by experiment and by simulation. Comparison of 2-D simulations of ITP and zone electrophoresis (ZE) confirms that ZE lacks the ability to resharpen protein zones after they pass through a T-junction.

Keywords:
2-D simulation / ITP / Microfluidic chip / Proteins / T-junction
DOI 10.1002/elps.200600525

1 Introduction

ITP is a well-known electrophoretic technique used in the separation of a variety of ionic compounds, ranging from small molecules like metal ions to large molecules like proteins. ITP is also a powerful sample preconcentration technique which is useful in the analysis of low abundance species. ITP has been successfully coupled with a number of analytical techniques, such as zone electrophoresis (ZE) [1, 2], IEF [3], LC [4], MS [5], Raman spectroscopy [6], and NMR spectroscopy [7, 8].

Analytical and preparative ITP of proteins has been extensively explored in gels and capillary tubes since the 1970s [9]. In an effort to replace conventional benchtop electrophoresis systems, microchip-based electrophoresis has received rapidly growing interest during the last decade because it has the potential to provide higher throughput, lower sample consumption, and lower fabrication costs. Although integration of ZE and IEF on microchips for protein separation shows a peak capacity comparable to 2-D PAGE [10, 11], protein detection is challenging due to the low sample mass loadings in a microfluidic chip. The best way to increase the loading capacity of a microfluidic chip is to preconcentrate the sample. Sample preconcentration is very important when analyzing biological samples which may have a large dynamic range of protein concentrations extending from the millimolar down to the femtomolar [12]. ITP is a simple and effective preconcentration and separation method which can be easily integrated on a chip prior to other on-chip operations, especially ZE.

As is the case with two other electrophoretic techniques, ZE and IEF, great progress has been made on the miniaturization of ITP. However, most of the published works on miniaturized ITP were focused on the separation of small organic molecules [13, 14] and metal ions [15, 16] which were primarily used in the food and beverage industry and for water analysis. ITP preconcentration and separation of proteins on chips has so far received relatively little interest.

In this work, we demonstrate ITP of proteins in a PDMS channel with T-junctions which we consider the key elements for the integration of unit operations, *e.g.*, sample loading. As briefly discussed in our previous work [17], dispersion of protein zones as they pass by a T-junction during electrophoresis is due to the deformation of electric field lines as current passes by the open channel. However, dis-

Correspondence: Dr. Cornelius F. Ivory, School of Chemical Engineering and Bioengineering, Washington State University, Pullman, WA 99164-2710, USA
E-mail: cfivory@wsu.edu
Fax: +**509-335-4806**

Abbreviations: APC, allophycocyanin; **EACA,** ε-amino-*n*-caproic acid; **GFP,** green fluorescent protein; **KRF,** Kohlrausch regulating function; **LE,** leading electrolyte; **MC,** methylcellulose; **PE,** *r*-phycoerythrin; **TE,** terminating electrolyte; **ZE,** zone electrophoresis

persion behaves differently in linear and nonlinear electrophoresis systems. To explore this difference in detail, a 2-D model of ITP was developed. 1-D ITP simulations are treated in detail in the works reported by Mosher *et al.* [9, 18] and 2-D simulations of linear electrophoresis (ZE) have been exhaustively investigated [19–21] but, to our knowledge, no 2-D simulations of nonlinear electrophoresis (ITP) have yet been reported aside from those briefly mentioned in our previous work, where ITP of a virtual protein was simulated in the domain of a single T-junction (Fig. 2 in [17]). In this paper, a 2-D ITP model is simulated using Comsol v3.2 (COMSOL, Burlington, MA), a finite-element based program that is widely available and easy-to-use. 2-D simulations are successfully used to explore the ITP features such as concentration stacking and self-sharpening of protein zones after they had been dispersed at a T-junction.

2 Materials and methods

2.1 Chemicals

Recombinant green fluorescent protein (GFP, MW ~ 28 000) was obtained from Upstate Biotechnology (Lake Placid, NY, USA). Allophycocyanin (APC, MW ~104 000) and *r*-phycoerythrin (PE, MW ~ 240 000) were purchased from Molecular Probes (Eugene, OR, USA). GFP, APC, and PE are naturally fluorescent. Methylcellulose (MC, viscosity of 2% aqueous solution at 25°C: 400 cP) and ε-amino-*n*-caproic acid (EACA, MW 131.2) were acquired from Sigma (St. Louis, MO, USA). Hydrochloric acid (HCl, MW 36.5) and Tris (MW 121.14) were purchased from Fisher Scientific (Fair Lawn, NJ, USA).

2.2 Electrolytes and protein sample solution preparation

The leading electrolyte (LE) solution was prepared by adjusting the pH of 10 mM HCl solution to 9.5 with Tris. The terminating electrolyte (TE) solution consists of 60 mM EACA titrated to pH 10.0 with Tris. The proteins PE, GFP, and APC were mixed and diluted in the LE solution to the concentrations of 0.03 μg/μL (1.25×10^{-4} mol/m^3), 0.06 μg/μL (2.14×10^{-3} mol/m^3), and 0.06 μg/μL (5.77×10^{-4} mol/m^3), respectively. All the solutions contain 2% w/v MC in order to suppress EOF [22].

2.3 Fabrication of PDMS microchips

The procedure used to fabricate PDMS chips was reported in our previous work [22]. Briefly, a positive pattern of the desired channel structure is formed on a glass substrate using a positive photolithography technique. PDMS prepolymer and curing agent (Sylgard 184, Dow Corning, Midland, MI, USA) were uniformly mixed in the ratio of 10:1, respectively, and degassed for 2 h at 0.001 Torr. The liquid elastomer is cast onto a positive pattern formed on the glass substrate and cured in a hot kiln for 6 h at 80°C. At the end of the curing process, the elastic polymeric material is carefully peeled from the glass substrate to form the bottom layer of the microchip. The open channel on this bottom layer is irreversibly sealed with a flat surface of another layer of PDMS substrate containing holes as reservoirs after both surfaces have been plasma-oxidized. This microchip (Fig. 1) consists of a straight channel and two secondary channels that branch out from the straight channel. All the channels are 300 μm wide and 10 μm deep.

2.4 ITP procedure

Initially, all the channels were pressure-filled with the LE from reservoir R_1 (Fig. 1). After all the reservoirs were cleaned by removing excessive LE, 30 μL of LE and 2% MC solution were loaded into R_1 and R_3, respectively. Protein sample solution was then carefully pressure-filled into the channel from reservoir R_4 at ~5 psi until a drop of liquid appeared at the channel entrance inside the reservoir R_2. Reservoir R_2 was cleaned and then loaded with 30 μL of TE. Reservoir R_4 was cleaned and then loaded with 2% MC solution. The reason for loading 2% MC solution into reservoirs R_3 and R_4 instead of leaving them empty is to balance the hydrostatic pressure among all the reservoirs. Figure 1 indicates the initial solution configuration usually obtained by this loading procedure. Platinum wire electrodes were immersed into reservoirs R_1 and R_2 while reservoirs R_3 and R_4 were left electrically floating. ITP was carried out at a constant voltage of 100 V using an XHR 600-1 power supply (Xantrex technology, Vancouver, Canada).

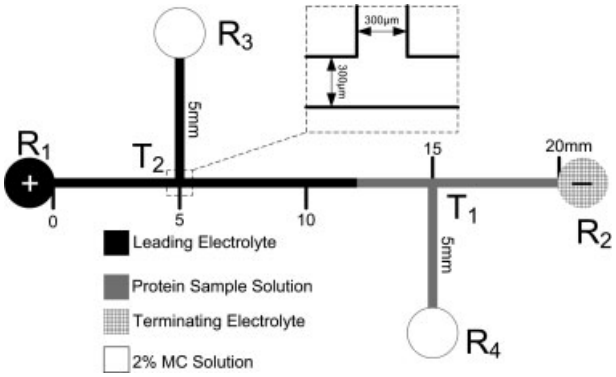

Figure 1. Schematic of the initial solution configuration in a microchip used in experiments. Please note that the protein sample solution is superimposed in the LE. R_{1-4} are reservoirs and T_{1-2} are T-junctions. Constant voltages are applied between R_1 and R_2 while R_3 and R_4 are left electrically floating. The length of the straight channel and branch channels are 20 and 5 mm respectively. The microchannel is 10 μm deep and 300 μm wide.

2.5 Imaging

The loaded chip was mounted underneath the 4 × objective lens of a Leica DMLB fluorescence microscope equipped with a CCD camera (SPOT RT color, Diagnostic instruments, Sterling Heights, MI, USA). The fluorescent proteins were excited with a mercury lamp (OSRAM HBO® 100 W/2) using a filter cube (DMLB 513804, Leica Microsystems, IL, USA). Electropherograms were obtained from the pixel intensities of the experimental images by using ImageJ (http://rsb.info.nih.gov/ij) to average the intensities across the channel width after subtracting the background signal intensity from the images.

2.6 Mathematical model

Under an external electric field, each charged species in a solution migrates by diffusion, electromigration, and convection. The flux of each species is given by the following equation:

$$J_i = -z_i F \mu_i C_i \nabla \Phi - D_i \nabla C_i + C_i u \quad (1)$$

where J_i is the flux of species i, C_i is the concentration of species i, F is the Faraday constant, z_i is the charge, μ_i is the absolute mobility, Φ is the electric potential, D_i is the diffusion coefficient, and u is the bulk flow velocity. The electrophoretic mobility (ω_i) is related to the absolute mobility by the following equation:

$$\omega_i = F z_i \mu_i \quad (2)$$

Each species is governed by the mass conservation law expressed as follows:

$$\frac{\partial C_i}{\partial t} = -\nabla \cdot J_i + R_i \quad (3)$$

where R_i is the rate of generation of species i.

Electroneutrality is conserved everywhere except inside the electric double layer which extends only to a few Debye lengths from the charged surface into the bulk solution. The microfluidic channels employed in our experiments are more than three orders of magnitude larger than the Debye length so, to a first approximation, the electroneutrality constraint can be applied everywhere on the scale of the microfluidic channel of interest, *i.e.*,

$$\sum z_i C_i = 0 \quad (4)$$

The current conservation equation is

$$F \frac{\partial \rho}{\partial t} + \nabla \cdot I = 0 \quad (5)$$

where ρ is the space charge density and the current is defined as $I = F \sum_i z_i J_i$.

Eq. (5) can be further simplified to

$$\nabla \cdot I = 0 \quad (6)$$

since $\rho = \sum_i z_i C_i = 0$ based on the electroneutrality equation.

2.7 Model simplification and setup

Some assumptions are made in the ITP simulation. First, z_i is assumed to be constant for each species everywhere in the microchip. The reaction term, R_i, in Eq. (3) is zero since the rate of generation of every species is nil. EOF is not included in this model since it was suppressed in the separation media that contains 2% w/v MC. However, if EOF exists, the ITP zones could decelerate or accelerate, achieve stationary steady state, or be flushed out of the separation channel, depending on the direction and strength of EOF [23]. The other forces that induce bulk flows, such as pressure differences among the reservoirs and electrical stresses are neglected and thus the bulk flow velocity, u, in Eq. (1) is taken to be zero.

The MC used to suppress the EOF increased the viscosity of the separation media but this is assumed to have no effect on the electrophoretic mobility of each species. The proteins used in the simulations are simply regarded as multiply charged molecules with electrophoretic mobilities between those of the leader and the terminator. Since the electrophoretic mobilities and charges of the proteins used in our experiments are not available in literature, three virtual proteins with multiple charges were used instead and were assigned electrophoretic mobilities between those of the leader and the terminator.

The Nernst–Planck physics built into Comsol v3.2 was employed to perform ITP simulations. A constant voltage was set on the boundary b1 (Fig. 2A) which is the entrance to the anode reservoir R_1 (Fig. 1) while zero voltage was set on the boundary b2 to be the cathode. The concentration of each species was fixed on boundaries b1 and b2. Since boundaries b3 and b4 are relatively far away from the main channel where ITP occurs, electric insulation and zero flux of each species were set on these two boundaries. All the channel walls are insulated to electric current and impermeable to species. Based on the initial solution configuration employed in the experiments, initial concentration profiles for LE, protein samples, and TE used in simulations are shown in Fig. 2B. The boundary conditions and initial conditions are summarized in Table 1.

3 Results and discussion

3.1 Experimental demonstration

The anionic ITP system employed in the experiments comprises the leading ion, chloride (10 mM HCl solution, adjusted to pH 9.5 by the addition of Tris), the terminating ion, EACA (60 mM EACA, titrated with Tris to pH 10.0), and a

Table 1. Boundary and initial conditions setup in simulations (COMSOL v3.2)

	Leading ion Cl^-	Protein sample	Terminating ion EACA	Counter-ion Tris	Voltage (V)
Boundary[a] (b1)	Concentration 10 mol/m^3	Concentration 0 mol/m^3	Concentration 0 mol/m^3	Electroneutrality[b]	0 V
Boundary[a] (b2)	Concentration 0 mol/m^3	Concentration 0 mol/m^3	Concentration 60 mol/m^3	Electroneutrality[b]	100 V
Boundary[a] (b3, b4)	Insulation	Insulation	Insulation	Insulation	Insulation
All other boundaries	Insulation	Insulation	Insulation	Insulation	Insulation
Initial condition[c]	$\frac{10\,\mathrm{mol/m^3}}{1+\exp\left(\frac{5(x-0.0195)}{0.001}\right)}$	$\frac{0.0005\,\mathrm{mol/m^3}}{1+\exp\left(\frac{-5(x-0.012)}{0.001}\right)+\exp\left(\frac{5(x-0.0195)}{0.001}\right)}$	$\frac{60\,\mathrm{mol/m^3}}{1+\exp\left(\frac{-5(x-0.0195)}{0.001}\right)}$	Electroneutrality[b]	N/A

a) Boundaries b1, b2, b3, and b4 are shown in Fig. 2.
b) Concentration of Tris was calculated on the basis of the electroneutrality equation (Eq. 4).
c) Variable *x* in the expressions for initial condition stands for *x*-axis which is the center line indicated in Fig. 2.

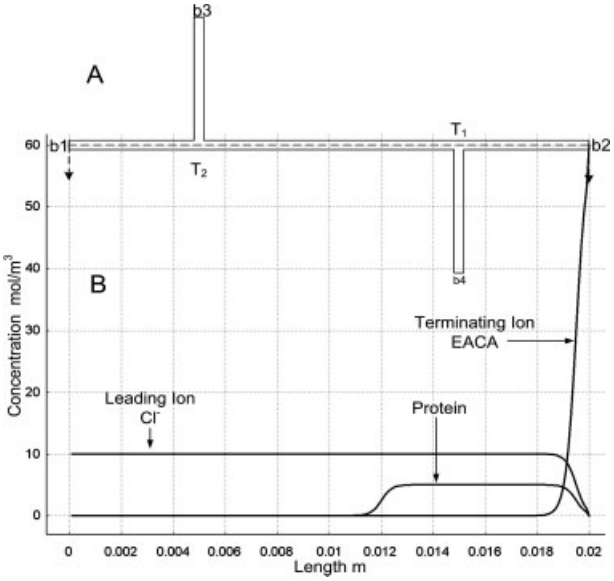

Figure 2. Domain and initial concentration profiles setup in COMSOL v3.2. (A) The geometry of simulation domain. (B) The initial concentration plot along the center line of the straight channel. For clarity, the protein concentration depicted in the plot is 10 000 times greater than the actual concentrations used in simulations.

mixture of three fluorescent proteins diluted in LE. Chloride is frequently used as a leader in anionic ITP since its electrophoretic mobility is higher than most of the other anions. Although EACA is relatively small in terms of molecular weight, it migrates slowly and acts as a terminator because it is partially ionized in pH 10.0 solution. Despite the large molecular weights, three fluorescent proteins are predicted to have electrophoretic mobilities between chloride and EACA due to multiple negative charges in the solution near pH 10.

The loaded protein sample covered nearly half the length of the straight channel while the remainder was filled with LE. As a constant voltage of 100 V was applied between anode and cathode reservoirs (Fig. 1), a bright-yellow edge formed at the entrance of the cathode reservoir and started to move toward the anode. The bright-yellow edge gradually separated into three adjacent zones with GFP in the middle as it approached the junction T1 (Fig. 3A). Experiments with a mixture of only PE and GFP under the same experimental conditions demonstrated that PE migrated isotachophoretically ahead of a green GFP zone. This indicated that three protein zones shown in Fig. 3 were PE, GFP, and APC respectively from left to right. Protein zones deformed when passing junction T1 (Fig. 3B), but they recovered their normal shape after migrating about 2 mm away from the T-junction. The three well-shaped protein zones shown in Fig. 3C were about 9 mm from the cathode reservoir. The total length of the three zones (Fig. 3C) increased by about 50% when compared to that shown in Fig. 3A mainly because the proteins initially introduced in LE were stacked into the corresponding zones as ITP progressed.

When the protein zones passed the junction T2 (Fig. 3D), deformation occurred again. The protein zones shown in Fig. 3E were about 1.5 mm from the anode reservoir and the average length of each zone was about 200 μm which indicated that each protein sample was concentrated about 40-fold when compared to the initial sample zone (Fig. 2B) which was about 8000 μm long, assuming that all of the proteins were present in the protein zones. Figure 3E also shows that the GFP zone was plateau-shaped, a common feature of ITP while PE and APC zones were more Gaussian, primarily because the initial molar concentrations of PE and APC were much lower than that of GFP and insufficient to produce the plateau-like zones. Figs. 3a, c, and e, the electropherograms of Figs. 3A, C, and E, provide a better view of the shape development of GFP zone from peak to plateau.

In our experiments, ITP was performed with fixed voltages instead of a constant current. The electric field in the LE gradually decreased as the total passing current decreased because an increasing length of the channel is occupied by the low conductivity TE as ITP progresses. As a result of the decrease in electric field in LE, the phenomenon that leading

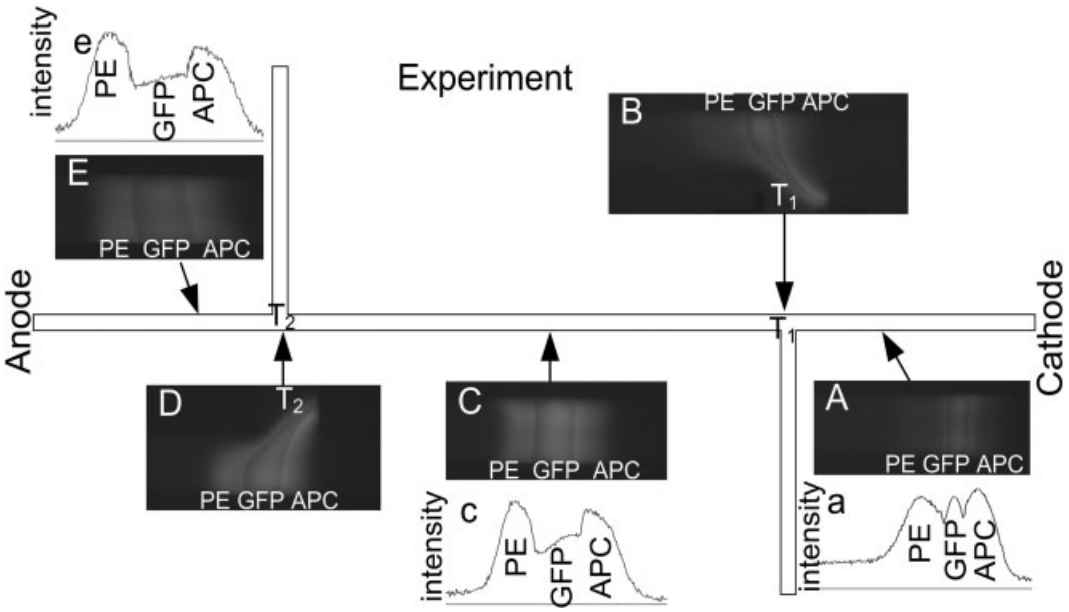

Figure 3. ITP stacking and separation of PE, GFP, and APC. (A) Protein zones are located between T_1 and cathode. (B) Protein zones are passing by T_1. (C) Protein zones are located between T_1 and T_2. (D) Protein zones are passing by T_2. (E) Protein zones are located between anode and T_2. (a), (c), and (e) are the electropherograms of (A), (C), and (E), respectively. Voltage, 100 V. All other experimental conditions are detailed in Section 3.1.

ion slowed down as ITP progress should be expected. This phenomenon was witnessed by observing the migration velocities of the leading and the terminating boundaries (Fig. 4A) since they were required by the ITP principle to migrate at the same velocity as the leading ion. The velocities of the moving boundaries were obtained at three different locations (Figs. 4A–C) along the channel in a single experiment. Figure 4A shows that the local average velocity of the moving boundaries was 20.4 μm/s since the terminating boundary took 49 s to migrate from the 8 to the 9 mm position mark. As the protein zones migrated further toward the anode, a deceleration was observed as revealed in Fig. 4B which indicated that the local average velocity of the moving boundaries was reduced to 17.5 μm/s. Furthermore, Fig. 4C shows that the leading boundary spent 6 s more as compared to that shown in Fig. 4B to travel the same distance (1 mm).

3.2 Simulation

In this work, numerical simulations were employed to help determine the underlying mechanisms for dispersion and resharpening. 2-D simulation of ITP is relatively straightforward using the Nernst–Planck physics built into COMSOL v3.2. The ITP model used in the simulation had seven variables of interest, the electric field, the concentrations of LE, three virtual proteins, TE, and the counter-ion. The Nernst–Planck physics utilized six equations of mass conservation (Eq. 3) and one electroneutrality constraint (Eq. 4) to solve for seven time-dependent variables.

The initial concentrations are depicted diagrammatically in Fig. 2. The protein samples were superimposed on the LE buffer and TE was interfaced with both LE and protein samples near the entrance to the cathode. Figure 5 depicts simulated concentrations of two virtual proteins at different times. The transport parameters for each species used in the simulations are listed in Table 2.

Figure 5A shows two small, overlapped peaks corresponding to protein 1 and 2 formed at the right end of the initial sample plug at 12 s. The initial protein samples ahead of these two peaks were also migrating toward the anode, but with speeds lower than the leading boundary and thus were being stacked into the corresponding peaks. At 150 s, two peaks had approximately 50% baseline overlap. The maximum concentration of protein 2 was more than 2-fold higher than that of protein 1 because more protein 2 was stacked into the corresponding peak than protein 1. This situation can be explained by the fact that protein 1 has a higher electrophoretic mobility than protein 2, and thus took a longer time to be caught up by the leading boundary. At 290 s, two peaks still had about 40% baseline overlap which suggests that a steady state had not yet been achieved within the sample zone. The peak heights of two proteins, especially protein 2 at 290 s were reduced when compared to those at 150 s due to the loss of proteins into the junction T_2 when the sample zone was passing by it.

Figure 5B shows the same simulation as Fig. 5A except for the change of the electrophoretic mobilities of two virtual proteins (Table 1). The peak baseline overlap was dramati-

Table 2. Parameters of each species used in simulations

	Leading ion Cl^-	Simulation A			Simulation B			Terminating ion EACA	Counter-ion Tris
		Protein 1	Protein 2	Protein 3	Protein 1	Protein 2	Protein 3		
Concentration mol/m^3 (C_i)	10	5×10^{-4}	5×10^{-4}	5×10^{-4}	5×10^{-4}	5×10^{-4}	5×10^{-4}	60	Electro-neutrality[a)]
Absolute mobility[b)] $\times 10^{-14}$ m^2/V·s (μ_i)	82.0	2.19	0.62	1.11	2.59	0.17	1.11	32.5	30.6
Diffusion coefficient[c)] $\times 10^{-11}$ m^2/s (D_i)	202.4	5.41	1.54	2.75	6.4	0.43	2.75	80.2	75.7
Charge (z_i)	−1	−26	−30	−28	−26	−30	−28	−0.15	0.96
Electrophoretic mobility $\times 10^{-8}$ m^2/V·s (ω_i)	7.91	5.5	1.8	3.0	6.5	0.5	3.0	0.47	2.84

a) Concentration of Tris was calculated based on the electroneutrality equation (Eq. 4).
b) Absolute mobility was calculated based on Eq. (2).
c) Diffusion coefficient is calculated based on the Einstein expression: $D_i = \mu_i RT$, where R is the gas constant 8.314 J·K^{-1} mol^{-1} and T is the room temperature 298 K.

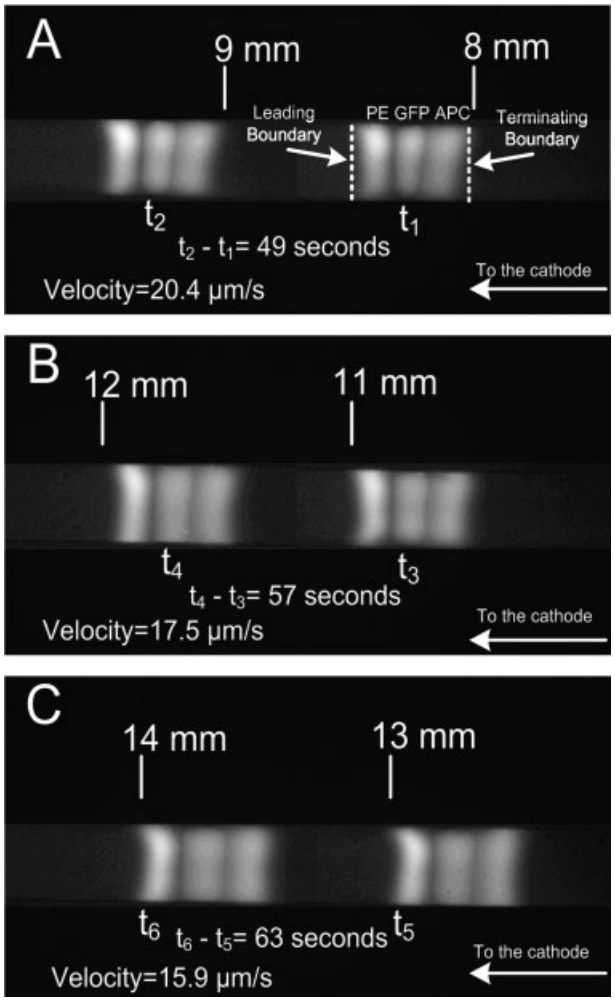

Figure 4. Measurement of isotachophoretic velocities in a single experiment at different locations. t_1–t_6 are the times after the electric field is applied. Protein zones are moving to the left. The velocity indicated in each photo is the local average velocity that is calculated on the basis of the time difference and the distance between two position markers. Voltage applied, 100 V. All other conditions are detailed in Section 3.1.

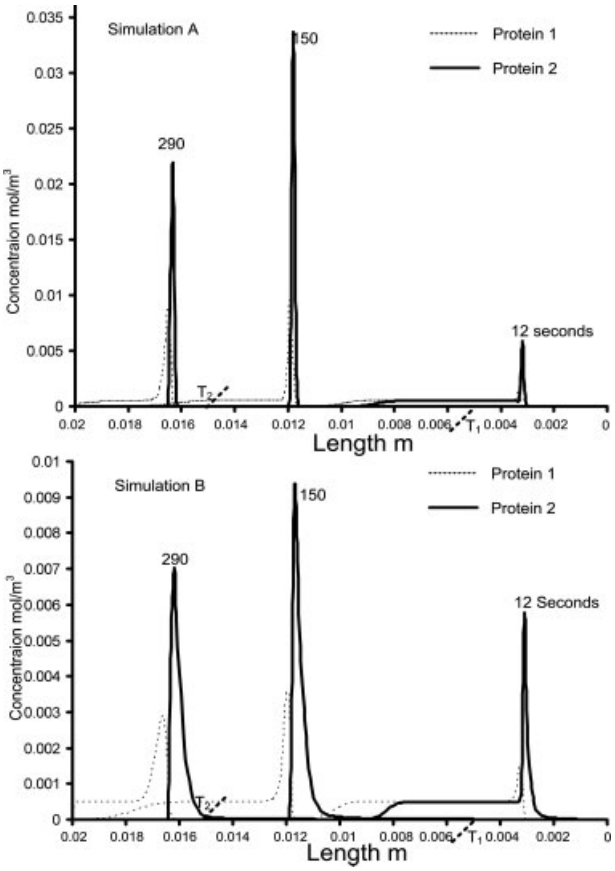

Figure 5. Simulation of virtual proteins with different electrophoretic mobilities. For clarity, only two virtual proteins are plotted in this figure. The parameters for each species are listed in Table 1. Simulation voltage, 100 V. Three sets of peaks shown in each plot represent the concentration profiles at three times during ITP simulation. Cathode is to the right.

cally reduced when compared with that shown in Fig. 5A due to an increase in the electrophoretic mobility difference between the two proteins.

The simulation above could potentially be used in chip design. For example, the length of the microchannel could be increased to allow all proteins to be stacked into their corresponding zones. It is convenient to explore ITP features, such as concentration stacking and moving boundaries, by means of numerical simulations. However, all the simulations of ITP in the literature including "The Dynamics of Electrophoresis" [9] are limited to 1-D. The 2-D simulation developed in this work provides a better way to explore some ITP features, such as the dispersion and self-sharpening of a protein zone both during and after passing a T-junction which will be discussed in the following paragraph.

3.3 Behavior of protein zones both during and after passing a T-junction

In the later part of the ITP experiment, the sharpened leading boundary of a moving zone of proteins (Fig. 6A) approached a T-junction (T_2 in Fig. 1). The upper part of the leading boundary was stretched up and sharply twisted as it was drawn about 150 μm (Fig. 6B, roughly half the channel width) into the junction channel while the lower part continued to move to the right, stretching and dispersing as it crossed T (Fig. 6C). The trailing zone boundaries then catch up with the top of the leading boundary and execute the same maneuver (Fig. 6C). After the protein zones have left the vicinity of the junction, Fig. 6D shows that the PE zone has re-resharpened, the GFP zone took on a trapezoid shape and was in the process of re-sharpening while the upper part of APC zone was still dispersed. As the protein zones migrated farther from the T-junction (Fig. 6E), they eventually finished re-sharpening with slightly tilted boundaries. Figures 6D and E also show that a very small amount of protein was left in the junction channel because it diffused too deep into the junction channel.

The primary source of dispersion at a T-junction in both linear and nonlinear electrophoresis is deformation of the electric field lines. This dispersion behaves differently in linear and nonlinear systems both while and after they pass the T-junction. In particular, nonlinear systems like ITP eventually resharpen the dispersed zone as shown in Figs. 6 F–J while zones in linear systems like ZE lack the ability to resharpen as illustrated in Figs 6 K–O.

To clearly explain the self-resharpening ability of ITP, it is necessary to mention the Kohlrausch regulating function (KRF) which is well defined elsewhere [9, 24, 25]. The KRF describes the local concentration of each charged species based on the initial concentration distribution along the electrophoretic axis and the value of KRF is not changed by the applied current [9]. Dilute species, *e. g.*, proteins in ITP experiments, are concentrated into narrow zones in order to maintain the higher concentration which is required by KRF. After an application of the electric field, mixed sample species separates based on their electrophoretic mobilities into a series of contiguous zones, demarcated by sharp moving boundaries [26]. The self-resharpening ability of ITP is

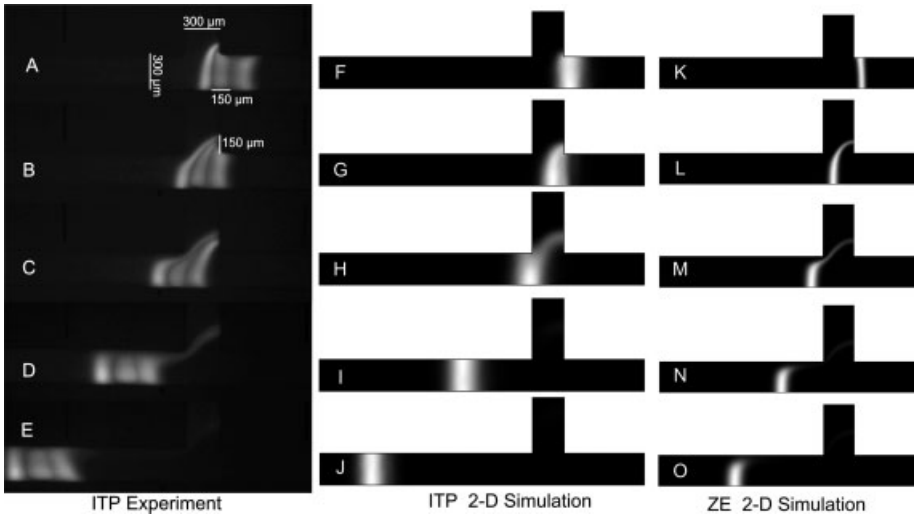

Figure 6. Time-series illustrations comparing band dispersion and resharpening by ITP and ZE at the T_2-junction of the PDMS microchip illustrated in Fig. 1. The time-series photos A–E show how an ITP train of three model proteins (PE, GFP, and APC) first disperses and then resharpens as it migrates straight through a T-junction. Figures F–J are part of an ITP simulation using three "virtual" proteins to illustrate how the ITP model mimics the essential mechanisms of dispersion and resharpening. Figures K–O, which are included only for the purposes of comparison with the ITP experiment and simulation, show that the morphology of dispersion at a junction is similar in ITP and ZE but that, in the latter case, the band cannot resharpen. Experimental conditions: R1 anode = 100 V; R2 cathode = 0 V; initial concentrations of LE, TE, and three fluorescent proteins are given in Section 3.1. Simulation results F–J and K–O are a comparison of ITP and ZE both during and after the bands pass the T-junction. ITP simulation is based on simulation B presented in Fig. 5. The ZE simulation has the same computing domain (see Fig. 2), species parameters and simulation voltage as for ITP but different initial concentration profiles and boundary conditions.

primarily provided by the nonlinear factor which is the step change of conductivities across the moving boundary. The step change in conductivities produces the step change in electric field magnitudes between ITP zones. When a species diffuse out of its own zone, it will experience either higher or lower electric field magnitude which will force it to either accelerate or decelerate back into its own zone [26]. In our case, the upper part of the protein zone was dispersed by the T-junction and retarded into the termination ion zone where the electric field is higher, and thus was accelerated to rejoin the protein zone. Because ZE lacks nonlinear factors, such as conductivity discontinuity, the ZE sample zone was not able to resharpen itself and stayed dispersed after passing by the T-junction (Figs. 6 M–O).

4 Concluding remarks

ITP stacking and concentration of mixtures of three fluorescent proteins has been demonstrated in a microfluidic chip with two T-junctions. Protein samples initially introduced into the microfluidic chip were successfully stacked into adjacent zones with an estimated concentration 40 times higher than the initial concentration. A gradual reduction of the isotachophoretic velocity during ITP at a constant voltage was due to decreasing current observed as TE occupied more of the channel.

Simulation provided a convenient tool to analyze stacking and moving boundary profiles since these are difficult to obtain from experiments. 2-D simulations of ITP showed excellent agreement with the experimental zone dispersion and resharpening both during and after passing a T-junction. The resharpening of the protein zones demonstrated here is due to the step change of conductivities across the terminating boundary. Comparison of 2-D simulations of ITP and ZE indicated that linear electrophoresis (ZE) lacks the ability to self-sharpen.

This paper is based upon work supported by the National Science Foundation under grant no. CTS-0300802. The authors thank Nazmul Huda Al Mamun and Dr. Keisuke Horiuchi for chip fabrication. The use of the bright field fluorescence microscope, provided by the Center for Multiphase Environmental Research (CMER) at Washington State University, is gratefully acknowledged.

5 References

[1] Kaniansky, D., Marak, J., *J. Chromatogr.* 1990, *498*, 191–204.

[2] Kaniansky, D., Zelensky, I., Hybenova, A., Onuska, F. I., *Anal. Chem.* 1994, *66*, 4258–4264.

[3] Mohan, D., Lee, C. S., *Electrophoresis* 2002, *23*, 3160–3167.

[4] Hutta, M., Kaniansky, D., Kovalcikova, E., Marak, J. *et al.*, *J. Chromatogr. A* 1995, *689*, 123–133.

[5] Smith, R. D., Fields, S. M., Loo, J. A., Barinaga, C. J. *et al.*, *Electrophoresis* 1990, *11*, 709–717.

[6] Walker, P. A., Kowalchyk, W. K., Morris, M. D., *Anal. Chem.* 1995, *67*, 4255–4260.

[7] Korir, A. K., Almeida, V. K., Malkin, D. S., Larive, C. K., *Anal. Chem.* 2005, *77*, 5998–6003.

[8] Wolters, A. M., Jayawickrama, D. A., Larive, C. K., Sweedler, J. V., *Anal. Chem.* 2002, *74*, 2306–2313.

[9] Mosher, R. A., Saville, D. A., Thormann, W., *The Dynamics of Electrophoresis*, VCH, New York 1992.

[10] Li, Y., Buch, J. S., Rosenberger, F., DeVoe, D. L., Lee, C. S., *Anal. Chem.* 2004, *76*, 742–748.

[11] Herr, A. E., Molho, J. I., Drouvalakis, K. A., Mikkelsen, J. C. *et al.*, *Anal. Chem.* 2003, *75*, 1180–1187.

[12] Binz, P. A., Müller, M., Hoogland, C., Zimmermann, C. *et al.*, *Curr. Opin. Biotech.* 2004, *15*, 17–23.

[13] Grass, B., Hergenroder, R., Neyer, A., Siepe, D., *J. Sep. Sci.* 2002, *25*, 135–140.

[14] Grass, B., Neyer, A., Johnck, M., Siepe, D. *et al.*, *Sens. Actuators B* 2001, *72*, 249–258.

[15] Prest, J. E., Baldock, S. J., Fielden, P. R., Goddard, N. J. *et al.*, *J. Chromatogr. A* 2004, *1047*, 289–298.

[16] Prest, J. E., Baldock, S. J., Fielden, P. R., Goddard, N. J., Brown, B. J. T., *Microchim. Acta* 2005, *151*, 223–230.

[17] Cui, H. C., Horiuchi, K., Dutta, P., Ivory, C. F., *Anal. Chem.* 2005, *77*, 7878–7886.

[18] Mosher, R. A., Gebauer, P., Caslavska, J., Thormann, W., *Anal. Chem.* 1992, *64*, 2991–2997.

[19] Ermakov, S. V., Jacobson, S. C., Ramsey, J. M., *Anal. Chem.* 1998, *70*, 4494–4504.

[20] Griffiths, S. K., Nilson, R. H., *Anal. Chem.* 2000, *72*, 5473–5482.

[21] Lin, R. S., Burke, D. T., Burns, M. A., *Anal. Chem.* 2005, *77*, 4338–4347.

[22] Cui, H. C., Horiuchi, K., Dutta, P., Ivory, C. F., *Anal. Chem.* 2005, *77*, 1303–1309.

[23] Thormann, W., Zhang, C. X., Gaslavska, J., Gebauer, P., Mosher, R. A., *Anal. Chem.* 1998, *70*, 549–562.

[24] Kohlrausch, F., *Ann. Phys. Chem.* 1897, *62*, 209–239.

[25] Vreeland, W. N., Williams, S. J., Barron, A. E., Sassi, A. P., *Anal. Chem.* 2003, *75*, 3059–3065.

[26] Hanna, M., Simpson, C., Perrett, D., *J. Chromatogr. A* 2000, *894*, 117–128.

